# Geology of a hydrothermal upflow zone on the Endeavour Segment, Juan de Fuca Ridge

Monica Kerr-Riess

Undergraduate Senior Thesis
University of Washington
School of Oceanography
Box 357940
1503 NE Boat St.
Seattle, WA 98195
mriess@u.washington.edu

Running Header: Endeavour upflow zone geology

Non-Technical Summary

Hydrothermal systems are areas where seawater fills into cracks in the seafloor and then circulates downward until it is heated to temperatures of 300°C or higher, usually by subsurface magma, in the reaction zone. The hot water then moves upward quickly through channels called upflow zones. During this process many chemical elements are exchanged between the rocks and the seawater flowing through them to produce hydrothermal fluids. The chemical elements that are exchanged can indicate the temperature of the fluids flowing through them. The minerals that are formed in the rocks can indicate the chemical elements that enriched the hydrothermal fluids. Hydrothermal systems tend to build chimneys and deposit sediments rich in metals on the seafloor.

The upflow zone on the Endeavour Segment, Juan de Fuca Ridge, represents an extinct hydrothermal system that was raised up by faulting, exposing the interior. Submersibles and remotely operated underwater vehicles were used to explore the area and collect still images, video, and rock samples from the area. In this study, the rock samples were examined to determine which minerals were present and where they had been altered by the hydrothermal fluids. The video and still images were examined to determine where different types of geological features were present and to create a map of these features. The results suggest that chimneys were built but remained relatively small and the area covered by hydrothermal sediments was also very small. The minerals found indicate that this upflow zone was a short-lived hydrothermal system with high temperature fluids, ›300°C, emanating from the vents. This upflow zone exhibits the typical components of an extinct hydrothermal system and can be used to gain more information about how hydrothermal systems are constructed.

Acknowledgements

Special thanks to Deborah Kelley, Alden Denny, and Mitchell Elend for their assistance with the research, reviewing manuscripts, and creation of images. Funding for this research was provided by the University of Washington Department of Oceanography.

Abstract

Circulation of fluids through the ocean crust results in significant transfer of heat from the lithosphere, provides a variety of biological habitats, and hosts chemical reactions in both the crust and seawater. The composition of the crust changes as fluids move through it and hydrothermal circulation concentrates metals and other elements in the formation of seafloor hot spring deposits. At the southern end of the Endeavour Segment, Juan de Fuca Ridge, is an exposed upflow zone from an extinct hydrothermal system centered at 47.90°N, 129.13°W. The interior of this upflow zone has been exposed through faulting, allowing for examination using submersibles and remotely operated vehicles (ROV). Sonar data, rock samples, video and still images were used to determine geologic, morphologic, and mineralogic characteristics of the upflow zone. The goal of this study was to determine subsurface characteristics of the upflow zone and its areal extent along the ridge. The exposed upflow zone measures 125 m in length by 91 m in height and is hosted primarily in basaltic pillow lavas. Massive sulfides, altered basalts, and sulfide chimneys up to 10 m in height are present. The alteration shows enrichment in copper, iron, and zinc in the fluids, similar to other Endeavour Segment hydrothermal fields. Presence of chalcopyrite indicates high temperature fluid flow of at least 300°C. There is a well-defined upflow zone with highly lithified metalliferous sediments at the top of the cliff, overlain by highly altered massive sulfide. The well defined gradient between highly altered and unaltered material in the upflow zone indicates that the flow was highly focused. There is a notable lack of quartz, relatively small chimney size compared to other Endeavour Segment hydrothermal fields, a small area covered by metalliferous sediments, and unaltered plagioclase phenocrysts in the altered basalt samples. The alteration rind on the altered basalts is relatively thin, < 10 mm. These data suggest that the upflow zone was a short-lived hydrothermal system.

Circulation of fluids through the ocean crust results in significant transfer of heat from the lithosphere, provides a variety of biological habitats, and hosts chemical reactions in both the crust and seawater (Kelley et al. 2002). Hydrothermal systems are responsible for removing about 30% of the heat from the oceanic crust (Stein and Stein 1994). The composition of the crust changes as fluids move through it, and hydrothermal circulation concentrates metals and other elements in the formation of seafloor hot spring deposits (Hannington et al. 1995).

Since hydrothermal systems were discovered in 1979, investigation of ophiolite sequences, and samples recovered from drilling and dredging have been the primary source of information about how the subsurface feeder systems for vents (upflow zones) are constructed. However, ophiolite sequences are affected by metamorphism and tectonism during their emplacement on land (Embley et al. 1988). This may have caused changes in the minerals and geology of the rock body leading to erroneous conclusions about the actual development, sub-seafloor structure, and mineralogy of hydrothermal systems. Drilling and dredging provide only small spatial glimpses into upflow zones (i.e. drilling recovery is commonly 10-15% and dredge samples « 1 m across) and they do not produce viable cross-sectional views.

Examination of exposed upflow zones on the seafloor can lead to detailed information about the geology and mineralogy of the sub-seafloor portions of hydrothermal systems because they have not been affected as greatly by non-ridge-related tectonism and metamorphism (Embley et al. 1988). Exposed upflow zones are tectonic windows into the subsurface features of a hydrothermal system. The minerals that are formed in the rocks can indicate the chemical elements that enriched the hydrothermal fluids. The chemical elements that are exchanged can indicate the temperature of the fluids flowing through them.

The Endeavour Segment is a 90 km-long mid-ocean ridge at the northern end of the Juan de Fuca Ridge, with a full spreading rate of 6 cm/yr (Riddihough et al. 1984) (Fig. 1). The central section of the segment, a 25 km volcanic high with a steep-sided axial valley, contains five known hydrothermal fields. The axial valley is approximately 3 km wide at the southern end. The upflow zone is approximately 4 km south of the southernmost known hydrothermal field, Mothra (Fig. 1) (Kelley et al. 2001, Glickson et al. 2007). The Endeavour Segment is underlain by an axial magma chamber, which is approximately 1.9 km deep at the northern end and in the south deepens to 3.3 km beneath the upflow zone (Fig. 2) (Van Ark et al. 2007).

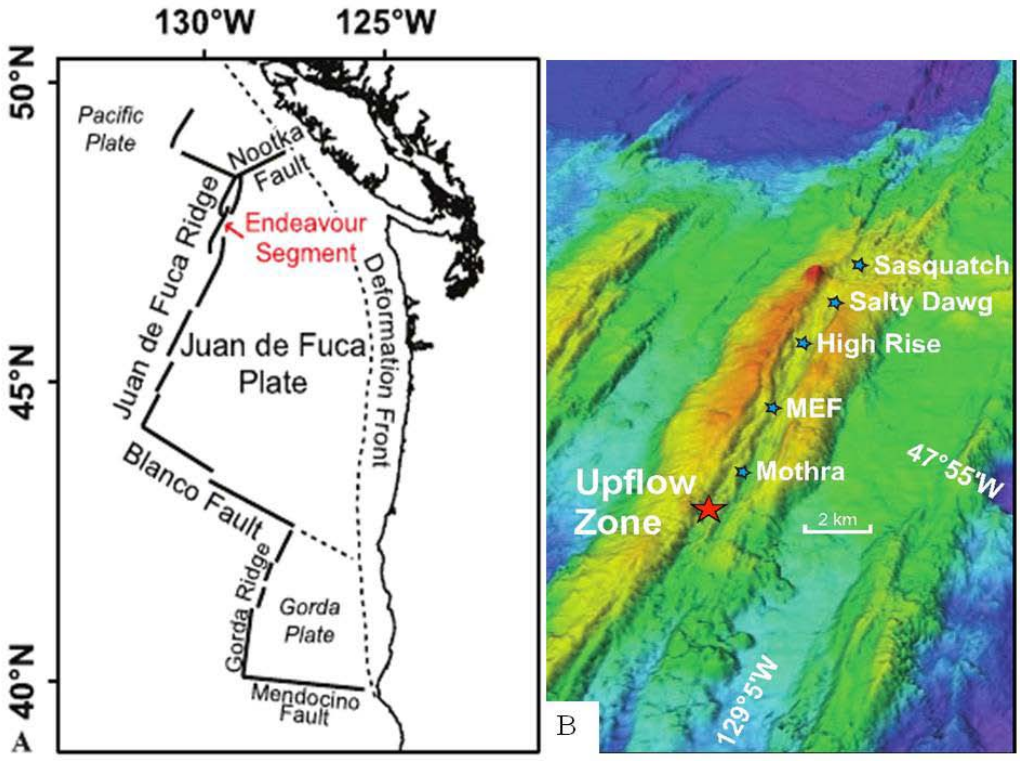


Figure 1: (A) Location of the Endeavour Segment of the Juan de Fuca Ridge. (Glickson et al. 2007). (B) EM300 and high resolution ABE bathymetry showing the central portion of the Endeavour Segment, the location of the five known hydrothermal fields, and the recently discovered upflow zone. Much of the axial valley depth in this area is ~2200-2300 m. Image courtesy D. Kelley.

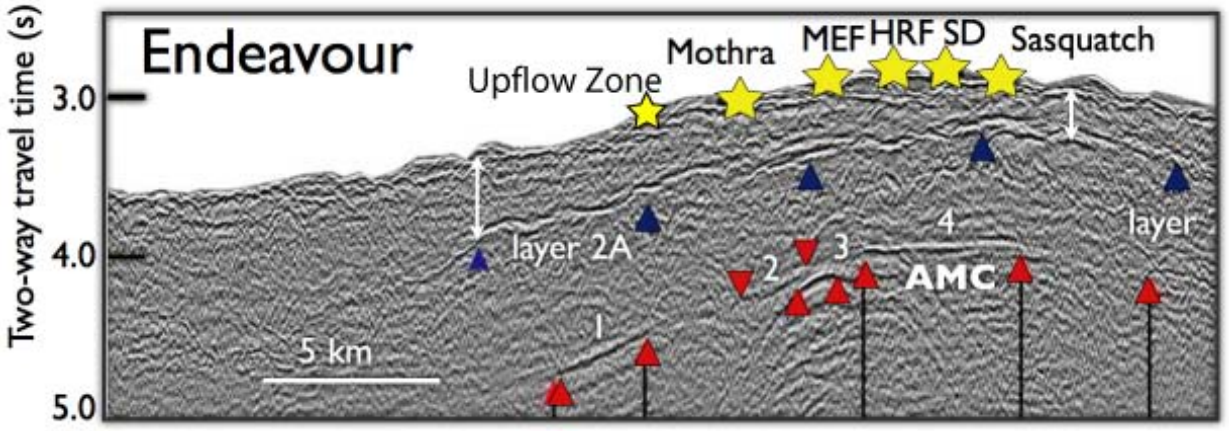


Figure 2: Location of the axial magma chamber under the Endeavour Segment. The red triangles outline the axial magma chamber, blue triangles outline layer 2A, and stars indicate the locations of the known hydrothermal fields and upflow zone.

At hydrothermal systems, seawater flows through cracks in the seafloor a distance away from the discharge area and slowly descends towards the heat source. Based on seismic data and location of vent fields, this heat source is a magma chamber underlying all five of the known fields at Endeavour (Van Ark et al. 2007). Once the fluids are heated in the reaction zone, at the base of the upflow zone, they ascend rapidly, at rates up to 0.56 m/s with focused flow through the upflow zone (Fig. 3) (Alt 1995).

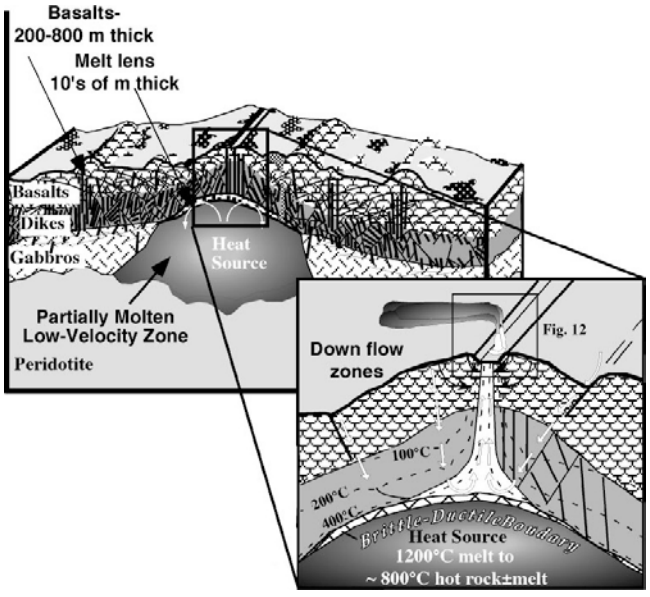


Figure 3: Theoretical diagram of the workings of a hydrothermal system. Cold seawater filters down away from the spreading center through small cracks in the rocks and sediments. As it gets deeper it heats up until it almost reaches the heat source. Once the fluids have reached the heat source they become buoyant and rise quickly through upflow zones (Kelley et al. 2002).

Previous studies of focused upflow zones have led to models of how these systems function. Temperatures are generally 300-400°C causing the loss of metals and sulfur from the rocks due to alteration by low pH hydrothermal fluids that become depleted in magnesium and sulfate (Alt 1995, Ridley et al. 1994). The rocks generally show Mg-enrichment and Ca-depletion (Ridley et al. 1994). In the Oman ophiolite, the rocks within upflow zones are altered with cloritic outer zones and illitic cores resulting in highly mineralized zones (Alt 1995). Studies of the Galapagos Fossil Hydrothermal Field (GFHF), an example of a rare exposed upflow zone along the Galapagos Ridge, indicate that the amount of alteration was directly proportional to the permeability of the rock (Embley et al. 1988). The altered rocks were depleted in Ca, K, and Na and enriched in Fe and S (Embley et al. 1988). The basalts showed zoned concentric alteration with rims the most altered, and less altered cores (Ridley et al. 1994). It is suggested that this was an open circulation system. Hydrothermal fluid mixing with warm seawater drove fluid-rock reactions as the fluids ascended and changed in composition prior to venting at the seafloor (Ridley et al. 1994). Other reactions that can occur during the upflow process include anhydrite precipitation, oxidation, smectite-chorite alteration rinds on pillow basalts, sulfate reduction, and precipitation of quartz (Table 1) (Alt 1995). The Sea Cliff hydrothermal field on the Gorda Ridge is an example of a diffuse flow hydrothermal field situated off-axis (Zierenberg et al. 1995). In this system most cations were removed from the basalts including sparingly soluble cations such as Al and Ti. The basalts were silicified. Mixing of hydrothermal fluids and shallow subsurface seawater were important in the alteration process (Zierenberg et al. 1995).

Table 1: Location and description of other studied upflow zones (Embley et al. 1988, Ridley et al. 1994, Hannington et al. 1995, Zierenberg et al. 1995).

| Name | Latitude | Longitude | Vertical Extent | Lateral Extent | Depth | Host Rock | Alteration Minerals | Inferred Temperature of Alteration |
|---|---|---|---|---|---|---|---|---|
| Gorda | 42° 44' N | 126° 43.7' W | 100 m total | | 2400 m | sediment | phyrrotite, isocubanite, chalcopyrite, sphalerite, arsenopyrite, and marcasite, anhydrite | 220° C + |
| GFHF | 00° 45' N | 85° 52' W | 30 m | 150 m | 2535 m | andesite | pyrite, chalcopyrite, sphalerite | up to 350° C |
| TAG | 26° 09'N | 44° 48' W | | | 3400 m | | chalcopyrite, pyrite, smectite, sphalerite | 290 - 320° C |

This paper presents the first characterization of an exposed upflow zone on the Endeavour Segment of the Juan de Fuca Ridge. Prior to this study, no exposed upflow zones had been discovered on the Juan de Fuca Ridge. Previous studies at the Endeavour Segment indicated a weak hydrothermal plume emanating from the western axial valley wall about 4 km south of the Mothra Hydrothermal Field (Pers. Comm. Kelley). For this study, the submersible Alvin was used to investigate these plumes and discovered the exposed upflow zone in 2006. In 2007 the ROV ROPOS returned to continue investigating this site. Based on preliminary observations, the upflow zone is an area approximately 125 m in length and 91 m high. The 91 m high wall contains altered basalts topped by lobate flows, metalliferous sediment, and extinct chimneys. Sonar data, rock samples, video and still images were used to determine geologic, morphologic, and mineralogic characteristics of the upflow zone and its extent. The purpose of this study was to map the exposures in detail along a 1700 m survey and delineate the extent of the upflow zone, the geology and tectonics of this area, and examine samples recovered during the dives in more detail. This exposure is only one of five investigated in the world's oceans and so study of this system offers a rare glimpse into these important seafloor features.

## Materials and Methods

The study area is centered at 47.90°N, 129.13°W and was examined during two dives. In 2006 the submersible Alvin was used to collect four hours of video, still images, and four rock

samples during R/V *Atlantis* cruise AT15-9. In 2007 the ROV ROPOS was used to collect 7.5 hours of video, still images, three sulfide, and seven basalt samples during the R/V *Thomas G. Thompson* cruise TN209. High resolution bathymetric data was obtained from an autonomous vehicle operated by the Monterrey Bay Research Aquarium in 2008. Mineralogy of cut hand samples was described based on observations with a dissecting microscope. All video was analyzed to determine the geologic setting of the upflow zone. Areas of unaltered and altered pillow basalts, unaltered and altered lobate flows, unaltered sheet flows, unaltered and altered talus, hydrothermal sediment, fissures, upflow, extinct chimneys, and sulfides were mapped at a minimum of 5 minute intervals throughout the video (Fig. 4). Excellent still images of each substrate type were catalogued. A spreadsheet to record the geologic features was developed and included the location, depth, heading, and description of the geologic features (Appendix 1). The geologic features were then categorized into one of the above categories and assigned a value in order to allow importation to ArcGIS. In ArcGIS both cruise tracks as well as all of the locations of the geologic features were plotted over the bathymetric data. Fault locations were inferred based on fissure locations, wall locations, and bathymetry.

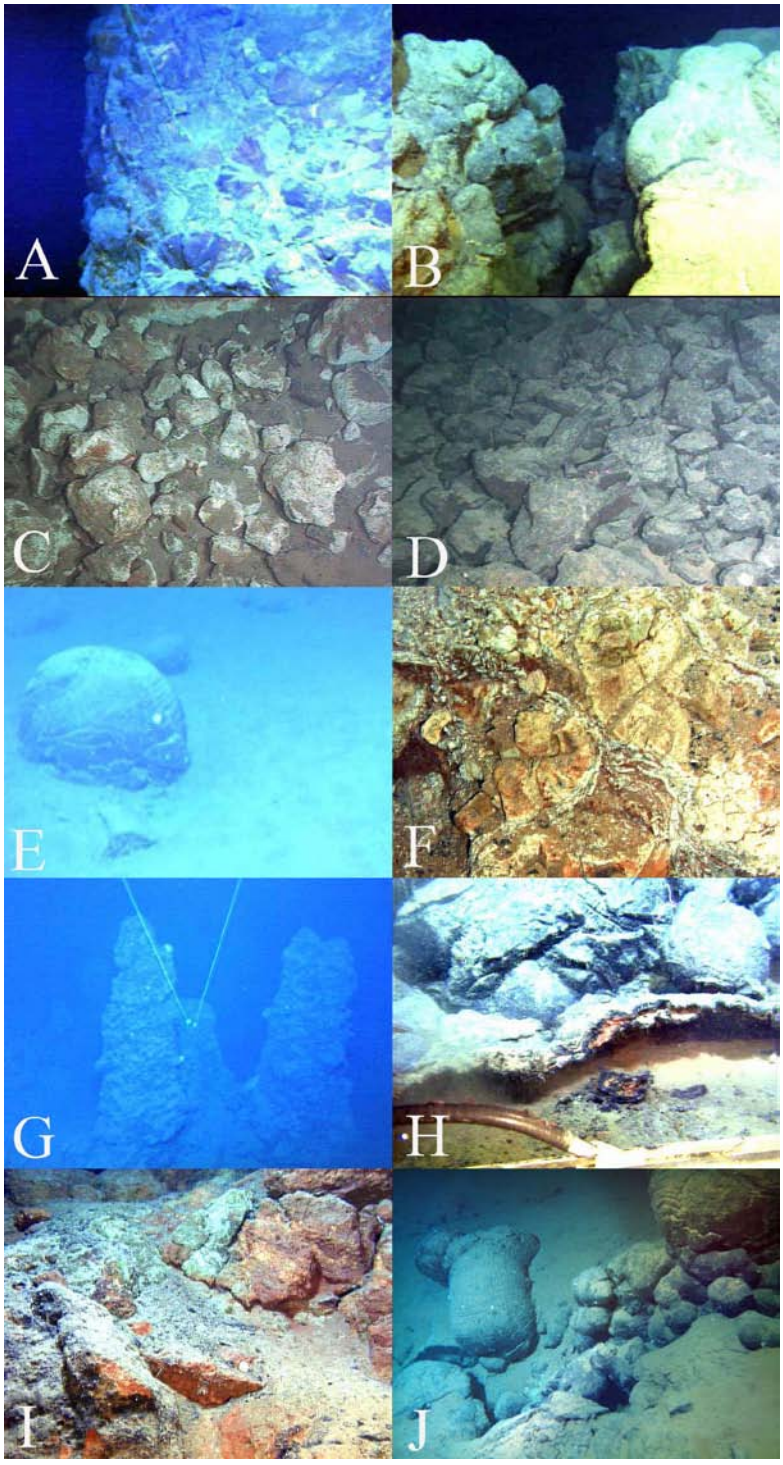


Figure 4: Geologic features present. Locations of each picture are shown in Fig. 6A. (A) Cliff edge (B) Fissure (C) Altered talus (D) Unaltered talus (E) Pillow basalt in heavy sediment (F) Altered basalt (G) Small chimneys (H) Drain-back basin (I) Sulfides (J) Lobate in heavy sediment.

Results

These data suggest that the exposed upflow area is 125 m long and 91 m high. A large fault runs along the exposure of the upflow zone. Additional faults and fissures are present, trending in a generally SW to NE direction. Within the upflow zone, the lower section is composed of highly altered basalts. The top several meters follow a progression of lobates, hydrothermal sediment, and massive sulfide mounds (Fig. 5). The base of the western axial valley wall consists of altered talus and the bounding basin to the east is covered by a thick layer of hydrothermal sediments with rare areas of outcropping pillow basalts, lobates, and extinct chimneys (Fig 4, 6). Many of the chimneys are still standing and range in height from 2-10 m. Additional chimneys have fallen over.

The area studied consists of two preserved upflow zones along the western axial valley wall, spaced about 1300 m apart, one at the northern end and the other at the southern end (Fig. 6). The northernmost zone is an extremely well exposed massive outcrop of truncated pillow basalts. The sides of the zone are well defined by an intense alteration gradient. In the core of the alteration zone the rocks are very light in color and show intense alteration, while a meter away the rocks are unaltered (Fig. 7). The pillow basalts within this zone average 0.5 m across and are highly altered on their outer surfaces. The alteration of the pillow basalts decreases towards the top of the wall. The top of the upflow zone is covered with thick metalliferous sediment overlaying pillow and lobate flows, sulfide blocks and rubble. At the southern end of the upflow zone medium-sized pillows and lobates are present, moving northward, sulfide blocks become the dominant feature, then returning to large pillow flows, and concluding with medium-sized pillows, lobates, and rubble (Fig. 5, 6).

The bounding basin to the east is covered by an anomalously thick layer of hydrothermal sediments. Rare outcroppings of pillow basalt and lobate flows occur. Rare chimneys of heights

up to 10 m are also present. In some areas the chimneys occur in small clusters of two to three. The base of the axial valley wall is marked by large amounts of angular basaltic talus, highly altered in areas near the upflow zones (Fig 6). The talus blocks are typically 0.2 – 0.8 m across.

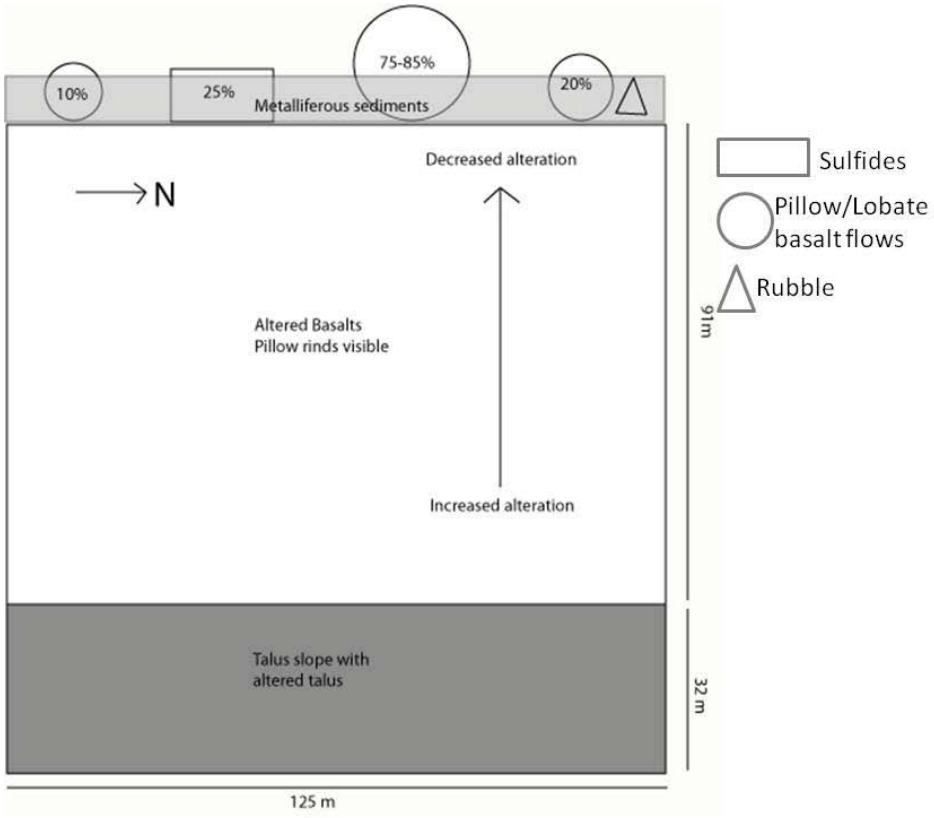


Figure 5: Layout of the wall of the northern upflow zone. At the base is a talus slope approximately 32 m in height, topped by 91 m of exposed upflow zone. The top of the upflow zone consists of pillow and lobate basalt flows, sulfide blocks, and rubble. The percentage abundance in each area is shown within the symbol. The length of the upflow zone is about 125 m. Depth of the top of the upflow zone is approximately 2188 m.

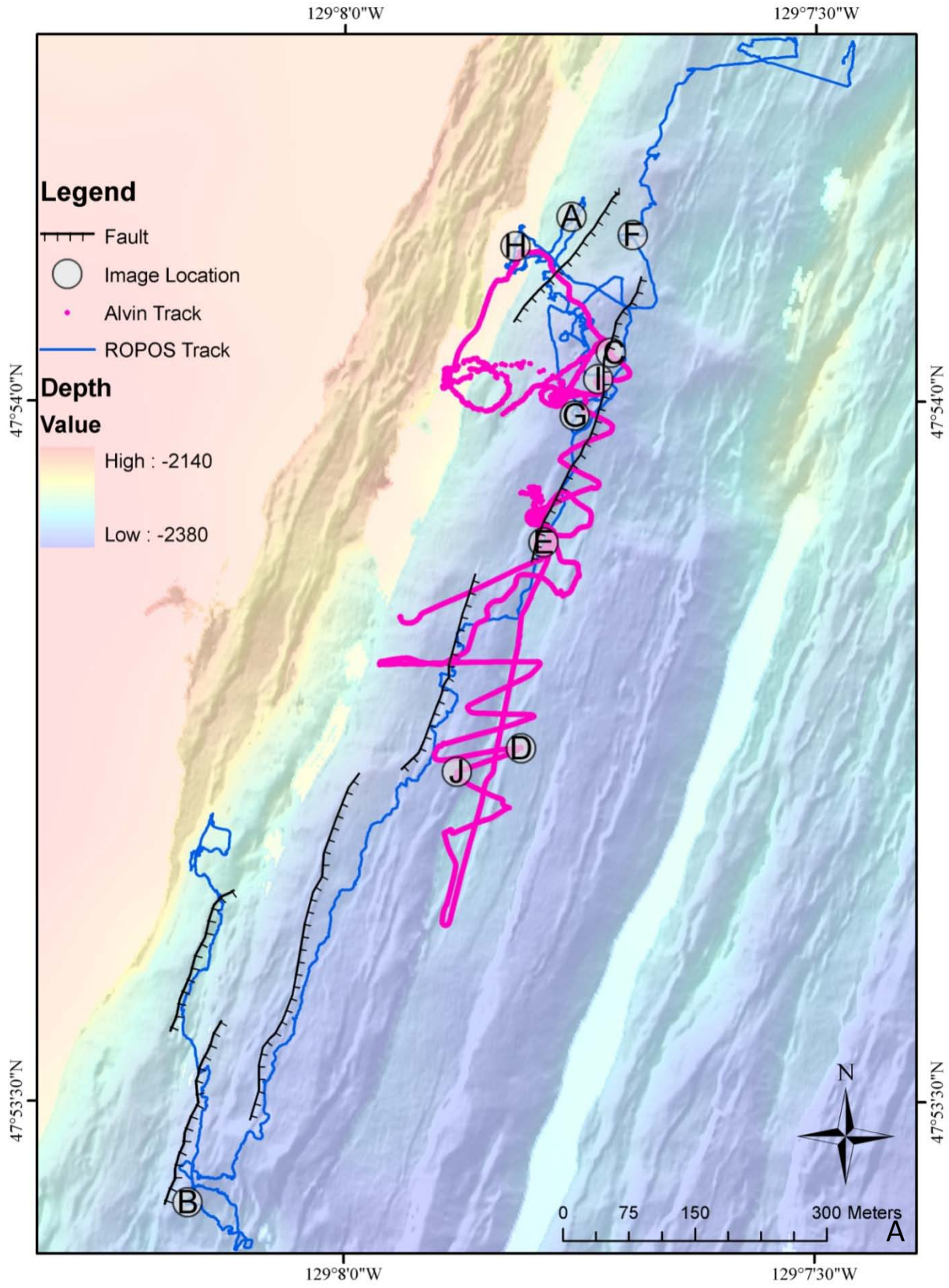
129°8'0"W
129°7'30"W
47°54'0"N
47°53'30"N
Legend
Fault
Image Location
Alvin Track
ROPOS Track
Depth
Value
High : -2140
Low : -2380
A
B
C
D
E
F
G
H
I
J
N
0
75
150
300 Meters
A

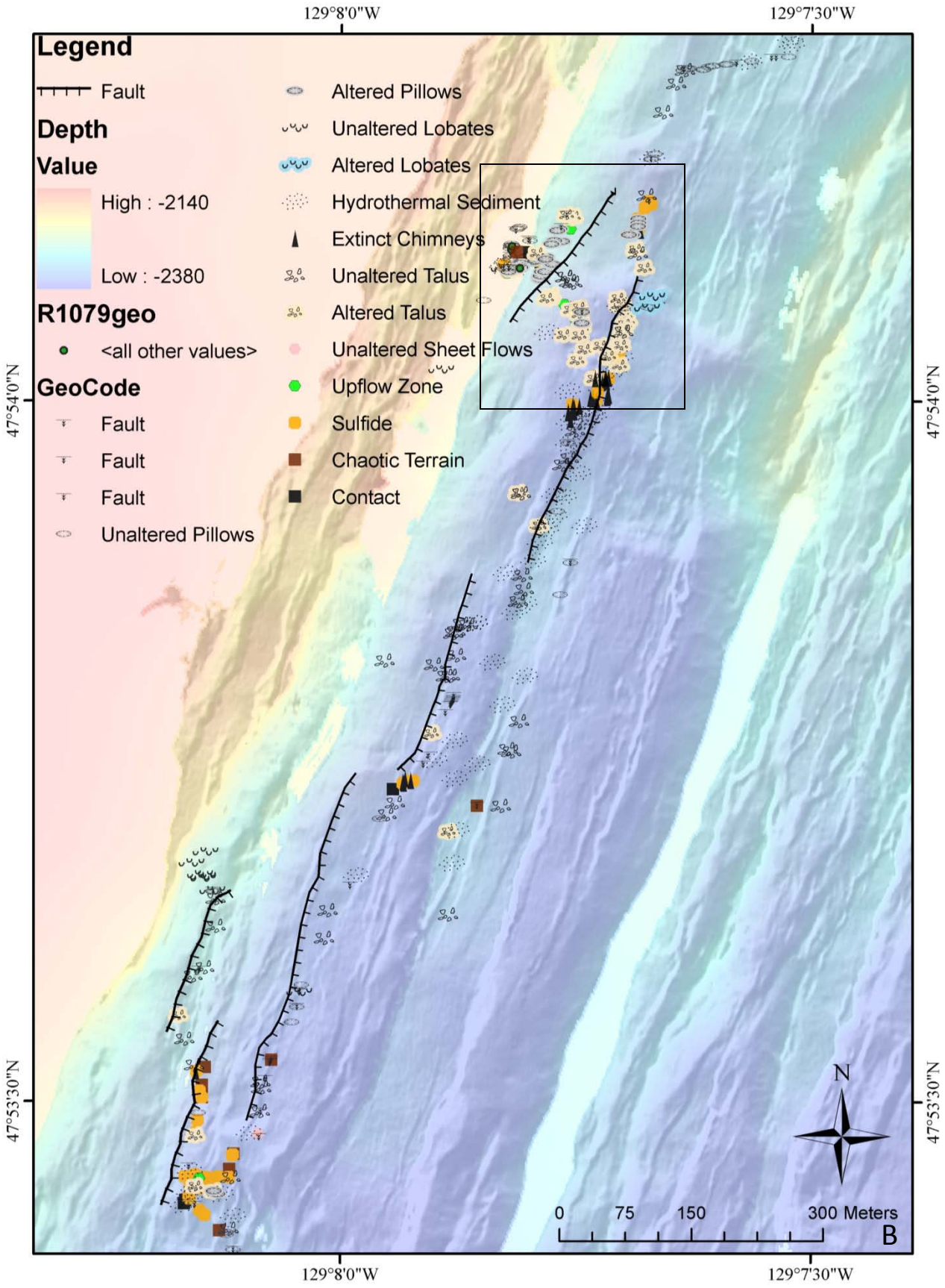
129°8'0"W
129°7'30"W
47°54'0"N
47°53'30"N
Legend
Fault
Depth
Value
High : -2140
Low : -2380
R1079geo
<all other values>
GeoCode
Fault
Fault
Fault
Unaltered Pillows
Altered Pillows
Unaltered Lobates
Altered Lobates
Hydrothermal Sediment
Extinct Chimneys
Unaltered Talus
Altered Talus
Unaltered Sheet Flows
Upflow Zone
Sulfide
Chaotic Terrain
Contact
N
0
75
150
300 Meters
B

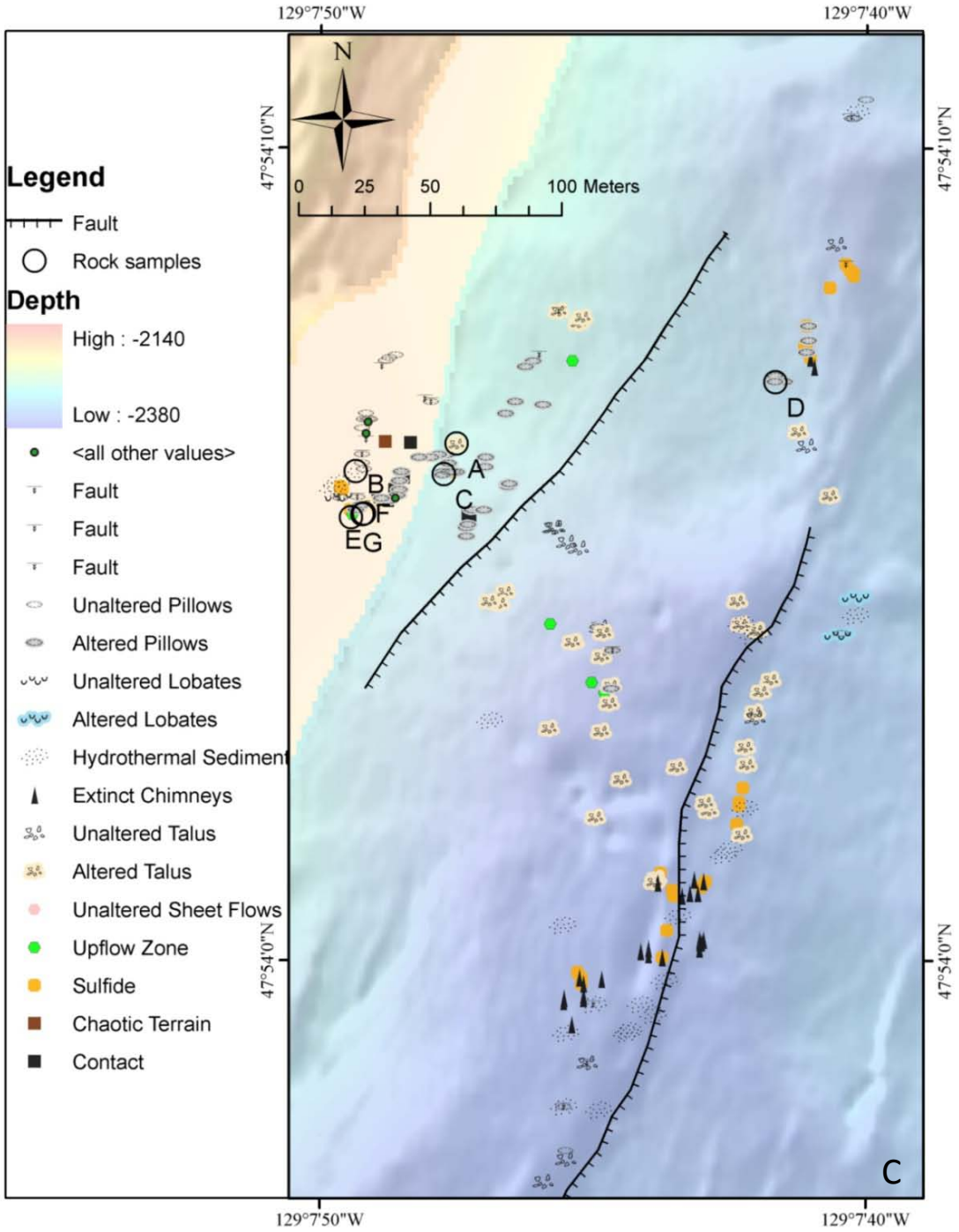


Figure 6: Map of the tracklines and geology covered by both the Alvin and ROPOS dives. Faults and depths are shown on all images. (A) The Alvin trackline is in pink and the ROPOS trackline is blue. Lettered symbols indicate the location of the images in Fig. 4. (B) Overview of the geologic features noted in the video. Boxed area shows northern upflow area enlarged in part C. (C) Detailed diagram of the geologic features in and near the northern upflow zone. The upflow zone exposure follows the fault in the northwest corner of the map. Lettered symbols indicate the location of the rock samples in Fig. 8.

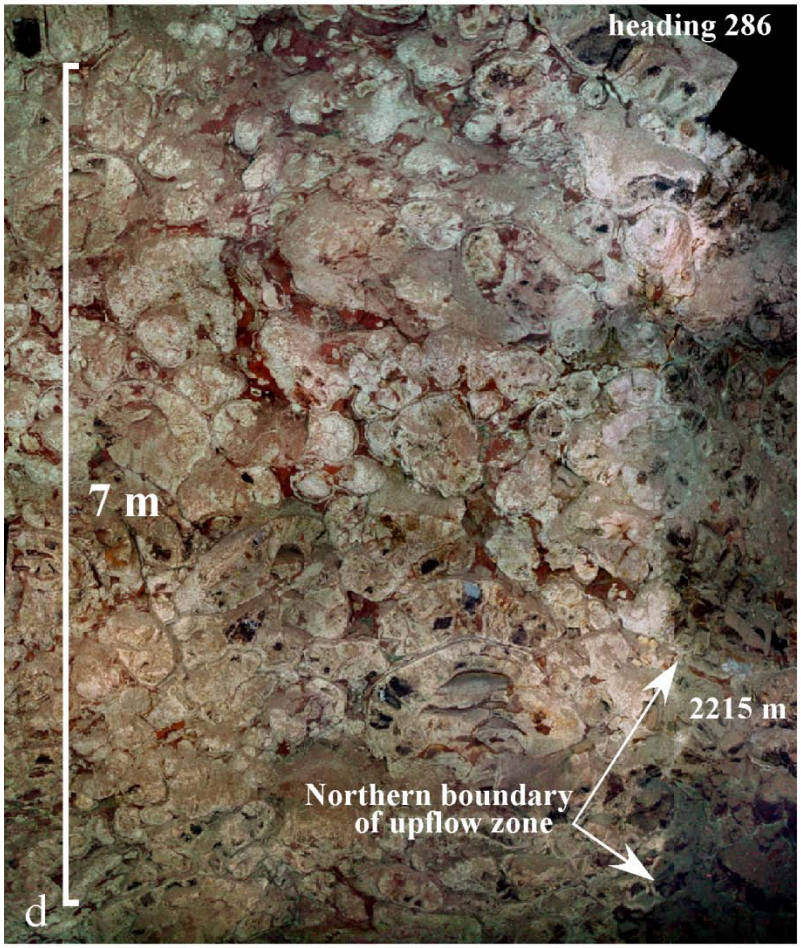


Figure 7: Mosaic of the wall showing the alteration boundary. The brighter left white/pink side is the altered basalt material. The darker right side is the unaltered material. The line between the two has been highlighted. Image courtesy of D. Kelley.

*Rock samples*

Sample R1079_0215 (Fig. 8) is a metal sulfide-rich rock and is highly porous. It is dominated by strand-like growths of pyrite, $FeS_{2,}$ and chalcopyrite, $CuFeS_{2,}$ with infilling sphalerite, (Zn,Fe)S, and anhydrite, $CaSO_4$. The exterior is a mixture of iron and copper oxide alteration products after chalcopyrite and pyrite as well as anhydrite. Alteration is to a depth of 1-2 mm and consistent around the sample. Pyrite, 30 modal %, consists of euhedral crystals growing into the pore spaces, otherwise the grains are subhedral to anhedral and ‹1 mm grain size with bright colored fresh faces. Crystals are oriented in an elongated fashion and alteration is present in only the exterior 1-2 mm. Sphalerite, 15 modal %, is subhedral to anhedral and

encrusts the pyrite/chalcopyrite matrix infilling the pore spaces, indicating that it was precipitated after the pyrite and chalcopyrite. Chalcopyrite, 10 modal %, is an amorphous conglomeration with elongated orientation. The grains are 1 mm and bright gold. Alteration products are only within 1-2 mm of the outer rim of the sample. Anhydrite, 5 modal %, consists of euhedral tabular crystals 2-3mm in size, infilling the pore spaces within the pyrite/chalcopyrite matrix and existing on the exterior. Pore space is 40% of the sample.

Sample R1079_0219 (Fig. 8) is a cryptocrystalline, phyric basalt with phenocrysts of plagioclase, $(Na,Ca)(Si,Al)_4O_8$. Rare narrow 15 mm fractures are lined with alteration and plagioclase crystals are altered when intersected by these fractures, and rarely cut by fine-grained pyrite. An alteration rind 4-15 mm thick consists of a soft white clay material with cryptocrystalline pyrite and chalcopyrite in dendritic patterns. The alteration rind is interpreted to result from pervasive alteration of the glassy pillow rind.

Sample A4245_1855 (Fig. 8) is a piece of sulfide breccia with a medium to coarse grained pyrite matrix and flowing strand like pyrite growths along the exterior 6-15 mm. The interior shows monomineralic chalcopyrite clasts 3-5cm in width. Medium to coarse grained pyrite is ubiquitous. The exterior contains 2mm, euhedral pyrite crystals as well as subhedral to anhedral, finer grained crystals. Also present are chalcocite, $Cu_2S$, and green copper oxide alteration minerals after pyrite. Pyrite, 30 modal %, is euhedral to subhedral grains ‹1 mm. The euhedral grains grow into pore spaces and exhibit brightly colored fresh faces. There is no visible alteration of the pyrite and the grains have an elongated orientation along the exterior 6-15 mm. Extremely fine-grained metal sulfides comprise 5 modal %. Chalcopyrite, 35 modal %, is amorphous and highly compacted. Pore space comprises 30% of the sample.

Sample R1079_0242 (Fig. 8) is a highly altered piece of massive sulfide with moderate pore space and a large cavity, 8 mm x 4 mm in size. Pores in the pyrite matrix are infilled with chalcopyrite, a light-green copper oxide, and brown-red iron oxide minerals. The exterior consists of Fe- and Cu- oxide alteration products of pyrite and chalcopyrite. An alteration rind 1-2 mm in thickness coats much of the outer surface, but is thinner in some areas. Pyrite, 60 modal %, forms euhedral grains within the pore spaces and is subhedral to anhedral elsewhere. Average grain sizes are ‹1 mm. The brown iron oxide comprises 5 modal %, is subhedral to anhedral filling pore spaces with ½ mm grains. The orange iron oxide, 3 modal %, is subhedral ½ mm grains infilling pore spaces. Chalcopyrite, 2 modal %, occurs with the brown iron oxide and consists of subhedral ‹½ mm grains. Pore space comprises 30% of the sample.

Sample R1079_0139 (Fig. 8) is a microcrystalline basalt with plagioclase phenocrysts and a finer grained matrix of plagioclase, pyroxene, and oxide minerals. The alteration rind is 1-7 mm thick and contains pyrite, chalcopyrite, and quartz. Secondary alterations occur along veins into the unaltered portions of the wall rock and are filled with pyrite.

Sample R1079_2335 (Fig. 8) is a cryptocrystalline basalt with an alteration rind of 6-9 mm. There are numerous altered cracks containing pyrite that extend into the unaltered interior of the sample. Numerous small voids ¼ - 1 mm in diameter are filled with euhedral crystals. Microcracks within the alteration rind are filled with bladed pyrite. Pyrite, plagioclase, and white clay material are dominant phases in the alteration rind.

Sample R1079_0217 (Fig. 8) is a cryptocrystalline basalt, phyric-poor, with an alteration rind ¼ - 1 mm in depth. The rind is generally separated from the unaltered area by a fracture and contains pyrite. The unaltered interior contains numerous voids ¼ to 1 mm in diameter, which are altered and small altered fractures run between the voids.

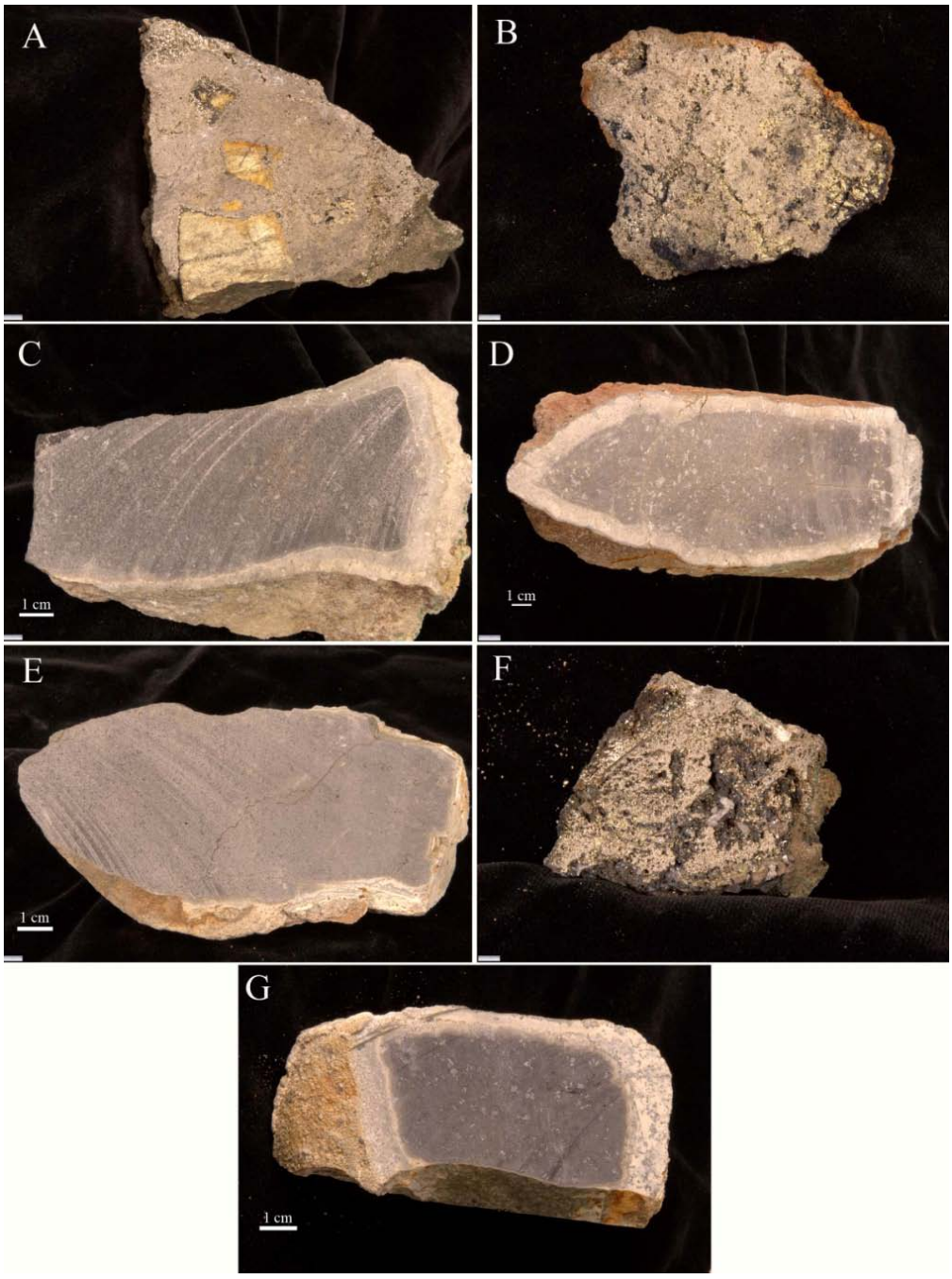


Figure 8: Rock samples showing cut faces. Location of each sample is shown in Fig. 6C. (A) A4245_1855, sulfide breccia showing large clasts of chalcopyrite in a pyrite matrix. (B) R1079_0242, highly altered massive sulfide consisting of a pyrite matrix infilled with chalcopyrite. (C) R1079_0139, microcrystalline basalt with plagioclase phenocrysts. Alteration rind is 1 – 7 mm thick. (D) R1079_2335, cryptocrystalline basalt with an alteration rind 6-9 mm thick. (E) R1079_0217, cryptocrystalline basalt with an alteration rind ¼ – 1 mm in depth. (F) R1079_0215, highly porous metal-sulfide rich rock containing pyrite, chalcopyrite, sphalerite, and anhydrite. (G) R1079_0219, cryptocrystalline basalt with plagioclase phenocrysts and an alteration rind 4 – 15 mm thick.

## Discussion

The northern upflow zone on the western axial valley wall exhibits all of the components of an extinct hydrothermal field. At the base of the cliff are extinct sulfide chimneys up 10 m in height. There is a well-defined upflow zone with highly lithified metalliferous sediments at the top of the cliff, overlain by highly altered massive sulfide. The well defined gradient between highly altered and unaltered material in the upflow zone indicates that the flow was highly focused. Similar rocks were found at a few locations along the base of the axial valley wall, indicating that there were probably one or two more of these systems on the axial valley wall across a distance of 1300 m. The faulting in the area was responsible for exposing this upflow zone for further study. A significant fault runs directly along the western axial valley wall and uplifted a portion of the hydrothermal field while leaving the other portion intact allowing for the examination of the interior of the system. Additional faulting reflects extension of the area.

The sulfide and altered basalt mineralogy indicate that the fluids flowing through the upflow zone were enriched in copper, zinc, and iron. The mineralogy is similar to sulfide chimneys elsewhere in the Endeavour system such as the Mothra and Main Endeavour systems (Tivey et al. 1999, Kristall et al. 2006). This indicates that the hydrothermal fluid chemistry may have been similar to fluids at the active vents in the Endeavor Segment (Butterfield et al. 1994). The fluids were probably quite different from the fluids that were venting at the GFHF, from which the mineralogy indicated fluids enriched in iron and sulfur (Embley et al. 1988). This suggests that the source rock or temperature of the fluids may influence the mineral enrichments of the fluids. At some point during the evolution of the upflow zones, the hydrothermal fluids were at least 300° C based on the presence of chalcopyrite (Kristall et al. 2006). Infilling of anhydrite into the pore spaces of the chalcopyrite/pyrite matrixes suggests that the temperatures

of the fluids may have been reduced as low as 150° C at some time after the formation of the matrix (Shanks et al. 1981). Most likely, this hydrothermal system experienced an earlier time of high temperature flow, ›300° C, followed by lower temperature flow, 150° - 300° C, at some later date.

Based on the small area covered by metalliferous sediments at the top of the upflow zone, lack of quartz in the hand samples, unaltered phyric plagioclase in the basalts, and relatively small chimney size, the upflow zone was a short-lived hydrothermal system. The capping sulfide deposits on top of the outcrop span a small area only a few meters across. The phyric plagioclase grains in the basalts were fresh indicating that only the outer rind of the basalts was altered. If the hydrothermal fluids had been flowing through the basalts for a long time the phenocrysts of plagioclase would have been altered. There is a notable lack of quartz in the rock samples. While other studied upflow zones, such as those at GFHF and the Gorda Ridge, contained significant concentrations of quartz, preliminary analyses indicates that this upflow zone is silica poor (Embley et al. 1988, Zierenberg et al. 1995). The Endeavour upflow zone consists of non-silicified basalts while the basalts at Gorda Ridge are all silicified, indicating a longer time of alteration at Gorda Ridge (Zierenberg et al. 1995). This supports the idea that the upflow zone was a relatively short-lived hydrothermal system. The chimneys at the base of the upflow zone are relatively small compared with chimneys at other Endeavor fields, particularly the Main Endeavor field, a longer lived system (Delaney et al. 1992). The chimneys at the Main Endeavor field are 50 m across and 30 m tall while the upflow zone chimneys are much smaller reaching a maximum height of 10 m (Delaney et al. 1992).

Due to the differences between this system and other exposed hydrothermal systems, additional study should be undertaken in order to determine the source of these differences. Bulk

rock chemistry and microprobe data could be used to analyze the rock samples which would allow for a better understanding of the circulation at this upflow zone as well as allowing for better comparisons between this and other exposed upflow zones in the world. Additional submersible or ROV exploration of the area would yield a better picture of the geology of the region and would allow for the collection of additional rock samples.

## Conclusion

The upflow zone at the Endeavour Segment provides a tectonic window into the plumbing of a hydrothermal system hosted in basaltic pillow lavas. It indicates that highly focused high temperature fluids ›300°C were venting at this site in the past. The duration of venting was relatively short due to the small chimney size, small area covered by metalliferous sediments, unaltered plagioclase phenocrysts in altered basalts, and lack of quartz in the rocks. The hydrothermal fluids were enriched in copper, iron, and zinc, typical enrichment for the currently active Endeavour Segment hydrothermal fields. Future study could yield more information about the rock chemistry and age of the system as well as obtaining a better picture of the layout of the system, allowing better comparison with other exposed upflow zones. These comparisons could lead to more detailed information about the causes of differences between the upflow zones.

References

Alt, J.C., 1995. Subseafloor processes in mid-ocean ridge hydrothermal systems. P. 85-114. *In* S.E. Humphris, R.A. Zierenberg, L.S. Mullineaux, R.E. Thomson [eds.], Seafloor hydrothermal systems: physical, chemical, biological, and geological interactions. AGU Geophysical monograph 91.

Butterfield, D. A., R. E. McDuff, M. J. Mottl, M. D. Lilley, J. E. Lupton, and G. J. Massoth. 1994. Gradients in the composition of hydrothermal fluids from the Endeavor Segment vent field - phase-separation and brine loss. Journal of Geophysical Research-Solid Earth **99:** 9561-9583.

Delaney, J. R., V. Robigou, R. E. McDuff, and M. K. Tivey. 1992. Geology of a vigorous hydrothermal system on the Endeavor Segment, Juan de Fuca ridge. Journal of Geophysical Research-Solid Earth **97:** 19663-19682.

Embley, R. W., I. R. Jonasson, M. R. Perfit, J. M. Franklin, M. A. Tivey, A. Malahoff, M. F. Smith, T. J. G. Francis. 1988. Submersible investigation of an extinct hydrothermal system on the Galapagos Ridge - sulfide mounds, stockwork zone, and differentiated lavas. Canadian Mineralogist **26:** 517-539.

Glickson, D. A., D. S. Kelley, and J. R. Delaney. 2007. Geology and hydrothermal evolution of the Mothra Hydrothermal Field, Endeavour Segment, Juan de Fuca Ridge. Geochemistry Geophysics Geosystems **8:** 23.

Hannington, M. D., M. K. Tivey, A. C. L. Larocque, S. Petersen, and P. A. Rona. 1995. The occurrence of gold in sulfide deposits of the TAG Hydrothermal Field, Mid-Atlantic Ridge. Canadian Mineralogist **33:** 1285-1310.

Kelley, D. S., J. R. Delaney, and D. R. Yoerger. 2001. Geology and venting characteristics of the Mothra hydrothermal field, Endeavour Segment, Juan de Fuca Ridge. Geology **29:** 959-962.

Kelley, D. S., J. A. Baross, and J. R. Delaney. 2002. Volcanoes, fluids, and life at mid-ocean ridge spreading centers. Annual Review of Earth and Planetary Sciences **30:** 385-491.

Kristall, B., D. S. Kelley, M. D. Hannington, and J. R. Delaney. 2006. Growth history of a diffusely venting sulfide structure from the Juan de Fuca Ridge: A petrological and geochemical study. Geochemistry Geophysics Geosystems **7**.

Riddihough, R. 1984. Recent movements of the Juan-de-Fuca plate system. Journal of Geophysical Research **89:** 6980-6994.

Ridley, W. I., M. R. Perfit, I. R. Jonasson, and M. F. Smith. 1994. Hydrothermal alteration in oceanic ridge volcanics - a detailed study at the Galapagos Fossil Hydrothermal Field. Geochimica Et Cosmochimica Acta **58:** 2477-2494.

Shanks, W. C., J. L. Bischoff, and R. J. Rosenbauer. 1981. Sea-water sulfate reduction and sulfur isotope fractionation in basaltic systems - interaction of sea-water with fayalite and magnetite at 200-350-degrees-C. Geochimica Et Cosmochimica Acta **45:** 1977-1995.

Stein, C. A., and S. Stein. 1994. Constraints on hydrothermal heat-flux through the oceanic lithosphere from global heat-flow. Journal of Geophysical Research-Solid Earth **99:** 3081-3095.

Tivey, M. K., D. S. Stakes, T. L. Cook, M. D. Hannington, and S. Petersen. 1999. A model for growth of steep-sided vent structures on the Endeavour Segment of the Juan de Fuca Ridge: Results of a petrologic and geochemical study. Journal of Geophysical Research-Solid Earth **104:** 22859-22883.

Van Ark, E. M., R. S. Detrick, J. P. Canales, S. M. Carbotte, A. J. Harding, G. M. Kent, M. R. Nedimovic, W. S. D. Wilcock, J. B. Diebold, J. M. Babcock. 2007. Seismic structure of the Endeavour Segment, Juan de Fuca Ridge: Correlations with seismicity and hydrothermal activity. Journal of Geophysical Research-Solid Earth **112:** 22.

Zierenberg, R. A., P. Schiffman, I. R. Jonasson, R. Tosdal, W. Pickthorn, and J. Mcclain. 1995. Alteration of basalt hyaloclastite at the off-axis Sea Cliff hydrothermal field, Gorda Ridge. Chemical Geology **126:** 77-99.

Appendix 1: Spreadsheet used to record the geologic features represented at 5 minute intervals throughout the Alvin dive. Spreadsheet includes the depth, vehicle's heading, vehicle's latitude and longitude, time, and a basic description of the geology at each location. A similar log was created for the ROPOS dive.

| DIVE# | DEPTH | DOP LAT | DOP LON | GYRO HDG | HH:MM:SS | COMMENTS |
|---|---|---|---|---|---|---|
| 4245 | | 47.89890177 | -129.1301435 | 288.1 | 15:23:00 | Reached bottom, 100% talus |
| 4245 | | 47.89890842 | -129.1301921 | 279.42 | 15:25:01 | talus 100%, slight alteration on some (5%) |
| 4245 | | 47.89891339 | -129.1301869 | 241.01 | 15:30:00 | talus 100%, slight alteration on some (5%) |
| 4245 | | 47.89750023 | -129.1318612 | 66.61 | 15:35:00 | bottom not visible |
| 4245 | 2299.405 | 47.89795293 | -129.1304135 | 66.73 | 15:40:00 | Heavy sediment over talus 100% |
| 4245 | 2311.649 | 47.89852294 | -129.1298205 | 288.07 | 15:45:01 | Heavy talus w/ moderate sediment 100% along wall |
| 4245 | | 47.89889046 | -129.129557 | 51.43 | 15:47:00 | Heavy sediment (100%) |
| 4245 | | 47.8985168 | -129.1290196 | 239.07 | 15:50:00 | heavy sediment (90%), talus (10%) |
| 4245 | | 47.89807843 | -129.1292668 | 102.54 | 15:55:00 | vertical wall with intact pillows, light sediment on wall, at least 20m high |
| 4245 | | 47.89769854 | -129.129445 | 260.02 | 16:00:00 | just passed the top of the wall, heavily sedimented w/intact pillows, possible slight alteration |
| 4245 | | 47.8979319 | -129.1301166 | 268.63 | 16:05:00 | Talus - 50% covered w/ heavy sediment 80% |
| 4245 | | 47.89736038 | -129.1309531 | 240.84 | 16:10:00 | Heavy sediment 100% |
| 4245 | | 47.8969734 | -129.131287 | 237.86 | 16:13:00 | Basalt talus 100% on wall |
| 4245 | | 47.89686496 | -129.131682 | 270.45 | 16:15:00 | Basalt talus 100% |
| 4245 | | 47.89690957 | -129.1325551 | 255.52 | 16:20:00 | Basalt talus 100% |
| 4245 | | 47.89686749 | -129.1320811 | 93.48 | 16:25:00 | bottom not visible |
| 4245 | | 47.89688466 | -129.131238 | 92.47 | 16:30:00 | bottom not visible |
| 4245 | | 47.89689254 | -129.1306472 | 90.88 | 16:32:00 | Heavy sediment 100% |
| 4245 | | 47.89672716 | -129.1300718 | 235.95 | 16:35:00 | Heavy sediment 100% over talus 10% |
| 4245 | | 47.89628043 | -129.1309216 | 96.54 | 16:40:00 | bottom not visible |
| 4245 | | 47.89619173 | -129.1301715 | 243.61 | 16:45:00 | Heavy sediment (100%) over talus (75%) |
| 4245 | | 47.89596351 | -129.1313083 | 245.05 | 16:50:00 | Heavy sediment (100%) over talus (25%) |
| 4245 | | 47.895728 | -129.1316699 | 96.64 | 16:55:00 | Heavy sediment (100%) over talus (25%) |
| 4245 | | 47.8958312 | -129.1307115 | 94.26 | 17:00:00 | bottom not visible |
| 4245 | | 47.8958605 | -129.1303775 | 93.61 | 17:02:00 | talus 90%, heavy sediment 10% |
| 4245 | | 47.89586999 | -129.1301965 | 136.45 | 17:04:00 | Basalt sample |
| 4245 | | 47.89583 | -129.1303128 | 249.54 | 17:05:00 | talus 50%, heavy sediment 50% |
| 4245 | | 47.89568467 | -129.1309105 | 238.4 | 17:10:00 | Heavy sediment (70%) lobates (30%) |
| 4245 | | 47.89550524 | -129.131315 | 136.5 | 17:15:00 | Very heavy sediment 100% |
| 4245 | | 47.89518214 | -129.1304966 | 135.74 | 17:20:00 | Talus 100% w/ light sediment |
| 4245 | | 47.89489062 | -129.1312749 | 240.63 | 17:25:00 | Heavy sediment (100%) over pillows (30%), 2 dropoffs |
| 4245 | | 47.89488058 | -129.1314235 | 341.85 | 17:26:15 | Altered seiments/basalts (white) occ. |
| 4245 | | 47.89450022 | -129.1313584 | 167.16 | 17:30:00 | heavy sediment 100% |
| 4245 | | 47.89389062 | -129.1314267 | 12.2 | 17:35:00 | talus 100% |
| 4245 | | 47.89518341 | -129.1309132 | 13.56 | 17:40:00 | heavy sediment 50%, talus 50%, wall, broken pillows |
| 4245 | | 47.89638536 | -129.1304695 | 8.29 | 17:45:00 | Heavy sediment 100%, over pillows 30% |
| 4245 | | 47.89758966 | -129.130086 | 29.57 | 17:50:00 | Heavy sediment 100% over pillows 40% |
| 4245 | | 47.89851622 | -129.1297607 | 295.08 | 17:55:00 | Heavy sediment 100% over pillows 20% |
| 4245 | | 47.89885611 | -129.1293885 | 69.93 | 18:00:00 | heavy sediment 100% over pillows 10% |
| 4245 | | 47.89914122 | -129.1291367 | 286.8 | 18:05:00 | heavy sediment 100% over pillows 5% |
| 4245 | | 47.89924369 | -129.1294134 | 286.69 | 18:06:30 | Talus 100% w/ medium sediment |
| 4245 | | 47.89948865 | -129.1291319 | 73.2 | 18:10:00 | heavy sediment 100% |
| 4245 | | 47.89981456 | -129.1288561 | 287.97 | 18:15:00 | heavy sediment 95% pillows 5% |
| 4245 | | 47.89993597 | -129.1291181 | 16.58 | 18:16:51 | extinct chimney |
| 4245 | | 47.90012011 | -129.1293165 | 260.21 | 18:20:00 | heavy sediment 75% over pillows 30% and lobates 10% |
| 4245 | | 47.90009017 | -129.1291388 | 84.51 | 18:25:00 | bottom not visible |
| 4245 | | 47.90010276 | -129.1287855 | 49.72 | 18:27:00 | sulfide |
| 4245 | | 47.90026456 | -129.1288325 | 87.04 | 18:29:15 | extinct chimney |
| 4245 | | 47.90027581 | -129.1286478 | 55.54 | 18:30:00 | same extinct chimney |
| 4245 | | 47.9004316 | -129.1284047 | 304.77 | 18:33:14 | altered talus 25%, unaltered talus 25%, heavy sediment 50% |
| 4245 | | 47.90046523 | -129.1284313 | 353.22 | 18:33:45 | sulfide mound |
| 4245 | | 47.90051283 | -129.128574 | 299.34 | 18:35:00 | altered talus 40%, unaltered talus 60% |
| 4245 | | 47.90053975 | -129.1285914 | 334.62 | 18:36:27 | altered talus 100% covered w/ moderate sediment |
| 4245 | | 47.90057909 | -129.1286249 | 323.53 | 18:37:45 | altered talus sample collected |
| 4245 | | 47.90066177 | -129.1287361 | 301.13 | 18:40:00 | altered talus 75%, unaltered talus 25%, covered w/ moderate sediment |
| 4245 | | 47.90106065 | -129.1290649 | 309.44 | 18:44:19 | wall of highly altered basalts |
| 4245 | | 47.90112042 | -129.129111 | 326.78 | 18:45:00 | altered talus 10%, unaltered talus 90% |
| 4245 | | 47.90168721 | -129.1297137 | 318.16 | 18:50:00 | massive sulfide (30%), collapse basin, altered basalts (70%) |
| 4245 | | 47.90176555 | -129.1298591 | 310.09 | 18:55:00 | altered talus 40%, unaltered talus 60%, sulfide sample collected |
| 4245 | 2199.327 | 47.90176896 | -129.1300943 | 262.86 | 18:58:15 | border between altered wall and unaltered wall |
| 4245 | | 47.90177243 | -129.1302225 | 330.78 | 19:00:00 | pillows (30%), lobates 10%, heavy sediment 40%, talus 20% |
| 4245 | | 47.90166593 | -129.1303046 | 247.52 | 19:05:00 | bottom not visible |
| 4245 | | 47.90158408 | -129.1303638 | 193.27 | 19:06:00 | altered basalts (10%), intact pillows, edge of wall |
| 4245 | | 47.9011996 | -129.1308068 | 196.07 | 19:10:00 | Heavy sediment 50%, pillows 50% |
| 4245 | | 47.90037336 | -129.1315645 | 223.67 | 19:15:00 | lobates (40%), pillows 10%, heavy sediment 50% |
| 4245 | | 47.90017517 | -129.1315934 | 4.35 | 19:18:00 | basalt sample |
| 4245 | | 47.90016148 | -129.1315728 | 9.5 | 19:20:00 | End of dive |